Published in final edited form as:
Glia. 2009 January 15; 57(2): 207–221. doi:10.1002/glia.20747.

Real-Time Passive Volume Responses of Astrocytes to Acute Osmotic and Ischemic Stress in Cortical Slices and *in vivo* Revealed by Two-Photon Microscopy

W. CHRISTOPHER RISHER[1], **R. DAVID ANDREW**[2], and **SERGEI A. KIROV**[3,*]

1*Graduate Program in Neuroscience, Medical College of Georgia, Augusta, Georgia*

2*Department of Anatomy and Cell Biology, Queen's University, Kingston, Ontario, Canada*

3*Department of Neurosurgery, Medical College of Georgia, Augusta, Georgia*

Abstract

The brain swells over the several minutes that follow stroke onset or acute hypo-osmotic stress because cells take up water. Measuring the volume responses of single neurons and glia has necessarily been confined to isolated or cultured cells. Two-photon laser scanning microscopy enables real-time visualization of cells functioning deep within living neocortex *in vivo* or in brain slices under physiologically relevant osmotic and ischemic stress. Astrocytes and their processes expressing green fluorescent protein in murine cortical slices swelled in response to 20 min of overhydration (-40 mOsm) and shrank during dehydration (+40 or +80 mOsm) at 32–34°C. Minute-by-minute monitoring revealed no detectable volume regulation during these osmotic challenges, particularly during the first 5 min. Astrocytes also rapidly swelled in response to elevated $[K^+]_o$ for 3 min or oxygen/glucose deprivation (OGD) for 10 min. Post-OGD, astroglial volume recovered quickly when slices were re-supplied with oxygen and glucose, while neurons remained swollen with beaded dendrites. *in vivo*, rapid astroglial swelling was confirmed within 6 min following intraperitoneal water injection or during the 6–12 min following cardiac arrest. While the astrocytic processes were clearly swollen, the extent of the astroglial arbor remained unchanged. Thus, in contrast to osmo-resistant pyramidal neurons (Andrew et al., 2007) that lack known aquaporins, astrocytes passively respond to acute osmotic stress, reflecting functional aquaporins in their plasma membrane. Unlike neurons, astrocytes better recover from brief ischemic insult in cortical slices, probably because their aquaporins facilitate water efflux.

Keywords

anoxic depolarization; volume regulation; osmolality; aquaporin

INTRODUCTION

Sudden disturbances in water balance can lead to the life-threatening state of brain edema (Fishman, 1975; Kimelberg, 2004). Brain cell swelling (cytotoxic/intracellular edema) quickly arises during stroke, brain trauma, or metabolic stress. A sub-type of intracellular edema is osmotic edema caused by acute dilution of the blood plasma. It is generated by a number of

*Correspondence to: Dr. Sergei A. Kirov, Department of Neurosurgery, Medical College of Georgia, 1120 15th Street, CB-3706, Augusta, Georgia 30912, USA. E-mail: skirov@mail.mcg.edu

Additional Supporting Information may be found in the online version of this article.

man-made situations within minutes, as follows forced water intake or overly aggressive rehydration of dehydrated patients. Conversely a rapid loss of water can follow infusion of mannitol to counteract brain swelling (reviewed in Andrew, 1991). Thus the conditions that rapidly swell or shrink mammalian brain cells are clinically important. Brain cell swelling can be indirectly measured as increases in extracellular resistance (Traynelis and Dingledine, 1989), field potential amplitude (Rosen and Andrew, 1990) or tissue light transmittance (Andrew and MacVicar, 1994). The development of 2-photon laser scanning microscopy (2PLSM) and transgenic mice with intrinsic fluorescent neurons and glia enables real-time study of cellular volume changes in brain slices and *in vivo* in settings relevant to clinical conditions.

When plasma osmolality rises or falls over many hours, brain cells regulate their volume by actively gaining or removing intracellular ions and organic substances (osmolytes) followed by osmotically obligated water (Chan and Fishman, 1979; Cserr et al., 1991; Finberg, 2000; Gullans and Verbalis, 1993; Pollock and Arieff, 1980). Within minutes or less, cultured or isolated brain cells are reported to compensate for sudden volume increases during extreme hypo-osmotic stress. However a regulatory volume decrease (RVD) by cells over such a brief period has not yet been confirmed *in vivo*. Until recently, it was not possible to monitor which cells were responsible for intact brain swelling. Using 2PLSM we showed that pyramidal neurons in cortical slices resist volume change during acute shifts in osmolality, likely because they lack functional aquaporins to conduct transmembrane water (Andrew et al., 2007). Nevertheless these same neurons swell and their dendrites bead within 5 min of anoxic depolarization (AD) both in slices (Andrew et al., 2007) and *in vivo* (Murphy et al., 2008). We proposed that astrocytes are primarily responsible for osmotic volume change by the brain whereas both neurons and astrocytes drive ischemic swelling of the gray matter.

Here we search for evidence of volume change and subsequent regulation by astrocytes in neocortical and hippocampal slices and *in vivo*. In slices the neuron—glia relationship and synaptic function are relatively intact. Furthermore the tissue is not constrained by cranium and dura, so it can recover from strong osmotic or ischemic challenge that might prove lethal *in situ*. We investigate several important questions at the level of the single astrocyte in real-time. Does astroglial volume change under osmotic or ischemic stress? Does RVD or regulatory volume increase (RVI) develop during physiologically relevant osmotic challenge? Do astrocytes and neurons differ in recovery from ischemia in cortical slices? Finally, can astroglial swelling under acute hypo-osmotic and ischemic conditions in cortical slices be confirmed in the intact mouse?

MATERIALS AND METHODS

Transgenic Mice

All procedures follow National Institutes of Health guidelines for the humane care and use of laboratory animals and underwent yearly review by the Animal Care and Use Committee at the Medical College of Georgia. All efforts were made to minimize animal suffering and to reduce the number of animals used. In total, 43 mice were used in this study. The founding mice of the FVB/N-Tg(GFAP-GFP)14Mes/J colony [GFAP-GFP] were purchased from Jackson Laboratories (Bar Harbor, ME). Mice of this strain display GFP fluorescence in astrocytes from multiple areas of the CNS (Supp. Info. Fig. 1A1) (Zhuo et al., 1997). The founding mice of the FVB/N-Tg(GFAP-EGFP)GFEA-FKi colony [GFAP-EGFP] were kindly provided by Dr. H. Kettenmann (Max Delbruck Center for Molecular Medicine, Berlin, Germany). The transgene in this strain labels astrocytes similarly to the GFAP-GFP strain, but EGFP fluorescence is brighter (Nolte et al., 2001). Founders of the B6.Cg-Tg(Thy1-YFPH) 2Jrs/J colony [YFP-H] were purchased from Jackson Laboratories and founders of the B6.Cg-TgN(thy1-GFP)MJrc colony [GFP-M] were kindly provided by Dr. J. Sanes (Harvard

University, Boston, MA). Mice of YFP-H and GFP-M strains display bright fluorescence in a fraction of pyramidal neurons of the neocortex and hippocampus (Feng et al., 2000). Hybrid mice, with a small proportion of both fluorescent neocortical and hippocampal pyramidal neurons and fluorescent astrocytes (Supp. Info. Fig. 1B1—B3), were generated by crossing between [GFAP-GFP] and [YFPH] or [GFP-M] strains. In some experiments astrocytes were labeled with the red astrocyte-specific stain sulforhodamine 101 (SR101; Invitrogen, Carlsbad, CA) (Nimmerjahn et al., 2004). A robust and specific labeling of astroglia (Supp. Info. Fig. 1A2) was achieved by topical application of SR101 to the exposed intact somatosensory cortex of the [GFP-M] mouse or the wild type littermate. It was anesthetized with an intraperitoneal (IP) injection of urethane (1.5 mg/g body weight) and 100 μM SR101 was applied through a craniotomy (around 2–3 mm diameter) with dura removed. After 20 min of application SR101 was washed out. The mouse was sacrificed 50 min later and slices made, using the standard protocol below.

Brain Slice Preparation and Solutions

Acute slices (400 μm) were made from 27 male and female adult mice at the average age of 5 months according to standard protocols (Kirov et al., 2004). Mice were deeply anesthetized with halothane and decapitated. The brain was quickly removed and placed in cold, oxygenated (95% O_2—5% CO_2) sucrose based artificial cerebrospinal fluid (ACSF) containing (in mM) 210 sucrose, 2.5 KCl, 25 $NaHCO_3$, 1 NaH_2PO_4, 8 $MgSO_4$,10 glucose, pH 7.4, 291–293 mOsm. Transverse slices, including hippocampus, subiculum, and neocortex, were cut from the middle third of the brain, using a vibrating-blade microtome (VT1000S, Leica Instruments, Nussloch, Germany). Immediately after sectioning the slices were submerged in standard ACSF bubbled with 95% O_2—5% CO_2 at room temperature. The standard (control) ACSF contained (in mM) 120 NaCl, 2.5 KCl, 25 $NaHCO_3$, 1 NaH_2PO_4, 2.5 $CaCl_2$, 1.3 $MgSO_4$, 10 glucose, pH 7.4, 291–293 mOsm.

Osmotic and ischemic changes in brain slices were sampled from neocortical layers II/III and V or the hippocampal CA1 region. All osmotic experiments started and ended in control (291–293 mOsm) ACSF. Osmolality was raised using mannitol or lowered by dilution with distilled water. Osmotic stress entailed a 15–20-min exposure to –40 and then +40 mOsm ACSF followed by return to control ACSF. Alternatively, slices were exposed to +40 and then –40 mOsm ACSF and then returned to control ACSF, or to +80 mOsm ACSF and then control ACSF. Some slices were prepared, pre-incubated, and osmotically stressed in the presence of 1 mM taurine, an amino acid reported to facilitate volume regulation (Kreisman and Olson, 2003). For oxygen/glucose deprivation (OGD) studies, N_2 replaced O_2 and glucose was lowered to 1 mM. NaCl was added to osmotically balance the removed glucose. Experiments began in control ACSF followed by a 10 min exposure to OGD ACSF. Re-oxygenation/normoglycemia was accomplished by returning to control ACSF bubbled with 95% O_2—5% CO_2. Experiments with high extracellular potassium ($[K^+]_O$) started and ended in control ACSF with a 3 min exposure to 26 mM K^+ ACSF (standard ACSF with 26 mM KCl replacing equiosmolar NaCl). All chemicals were from Sigma Chemical (St. Louis, MO) unless indicated otherwise.

In Vitro Live Imaging and Recording

After at least 1 h of incubation a slice was transferred into a submersion-type imaging/recording chamber (RC-29, 629 μL working volume, Warner Instruments, Hamden, CT) mounted on the Luigs & Neumann microscope stage (Ratingen, Germany). The ACSF was bubbled with 95% O_2—5% CO_2 and preheated before delivery into the chamber to prevent degassing. The slice was held down by an anchor (SHD-27LP/2, Warner) and perfused with oxygenated ACSF at 32–34°C, using a re-circulating system. The solution flow in and out of the chamber was controlled by two peristaltic pumps (Watson-Marlow, Wilmington, MA) set at the rate of 8

mL/min. At this rate it takes ~ 17 s to exchange solutions in the chamber. Temperature was monitored by a thermistor probe within 1 mm of slice and maintained by an in-line solution heater/cooler (CL-100, Warner) with a bipolar temperature controller (TA-29; Warner). Field excitatory postsynaptic potentials were recorded with MultiClamp 200B amplifier (Axon Instruments/Molecular Devices, Sunnyvale, CA) in the middle of *stratum radiatum* of some slices to confirm viability. Signals were filtered at 2 kHz, digitized at 10 kHz with Digidata 1322A interface board (Axon) and analyzed with pClamp 9 software (Axon). Evoked synaptic responses in healthy slices had a sigmoidal input/output response function and a stable response at ½ maximal stimulation.

Preparation of Mice for *in vivo* Imaging

Craniotomy for the open-glass optical window followed a protocol adapted from Holtmaat et al. (2005). A total of 16 adult GFAP-EGFP male and female mice at the average age of 4 months were anesthetized with an IP injection of urethane (1.5 mg/g). Body temperature was maintained at 37°C with a heating pad (Sunbeam, Boca Raton, FL). Skin covering the cranium above the somatosensory-cortex was removed. A custom-made 1.3 cm diameter plastic ring was glued with dental acrylic cement (Co-Oral-Ite Dental, Diamond Springs, CA) to stabilize the head with a mouse headholder (Fried et al., 2001) during craniotomy and imaging. A dental drill (Midwest Stylus mini 540S; Dentsply, Des Plaines, IL) with ¼ bit was used to thin the circumference of a 2–4 mm diameter circular region of the skull centered at stereotaxic coordinates -1.8 mm from bregma and 2.8 mm lateral. Forceps were used to lift up the thinned portion of the skull. An optical chamber was constructed by covering the intact dura with a thin layer of 1.5% agarose (prepared in a HEPES-buffered ACSF) and sealed by a circular coverglass (No. 1), using dental cement. Following installation of the window, the stage containing headholder, mouse, and heating pad was mounted on the Luigs & Neumann microscope stage for imaging. Mice were maintained under urethane anesthesia for the entire imaging session. Heart rate was monitored using DAM-60 amplifier (World Precision Instruments, Sarasota, FL). A 0.1 mL bolus of 5% (w/v) Texas Red Dextran (70 kDA) (Invitrogen) in PBS was injected into the tail vein for blood flow visualization. In a set of experiments global ischemia was induced by cardiac arrest (CA) resulting from 1 mL of air embolization into the tail vein. In a different set of experiments, over-hydration was accomplished by IP injection of distilled water (150 mL/kg) (Nagelhus et al., 1993).

Two-Photon Laser Scanning Microscopy

Images were collected with IR optimized 403×/0.8 NA or 633×/0.9 NA water immersion objectives (Carl Zeiss, Jena, Germany), using the Zeiss LSM 510 NLO META multi-photon system mounted on the motorized upright Axioscope 2 FS microscope (Zeiss). The scan module was directly coupled with the Spectra-Physics (Mountain View, CA) Ti:sapphire broadband mode-locked laser (Mai-Tai) tuned to 910 nm for 2-photon excitation. To monitor structural changes with GFP three-dimensional time-lapse images were taken at 0.5–1 μm increments, using 4X optical zoom, resulting in a nominal spatial resolution of 28 pixels/μm with a 63×/0.9 NA objective (12 bits per pixel, 2.24 μs pixel time). Emitted light was detected by internal photomultiplier tubes (PMT) of the scan module with the pinhole entirely opened or in a whole-field detection mode by external non-de-scanned detectors (Zeiss). Data acquisition was controlled by Zeiss LSM 510 software.

Image Analysis and Statistics

The LSM 510 Image Examiner software (Zeiss) was used together with NIH ImageJ (http://rsb.info.nih.gov/ij/) and Bitplane Imaris software (St. Paul, MN) for volume rendering and image analysis. A median filter (radius = 2) was applied to images in figures to reduce photon and PMT noise. Given the relatively poor axial resolution of 2PLSM (~ 2 μm), we

used two-dimensional Maximum Intensity Projections (MIPs) of image stacks for analyses. Such analyses assumed that astroglial soma volume is changing uniformly in all directions, based on viewing astrocytes along the *z*-axis before and after osmotic challenge. In this case, measurements of changes in the lateral dimensions were adequate to determine relative volume changes, which underestimated actual volume changes assuming they are approximately isotropic. We employed three techniques to measure relative volume changes (Andrew et al., 2007). (1) MIP images were digitally traced by hand to measure the area of astroglial and neuronal soma profiles in control and for each time point. (2) Control and experimental MIP images were pseudocolored green and red, aligned and overlaid. Overlapping areas projected as yellow, whereas different areas remained red or green. (3) Control profiles were traced and filled to create a mask, which revealed peripheral areas of swelling when overlaid upon experimental images.

Using plasma membrane-impermeant fluorescent probes in culture, Crowe et al. (1995) measured changes in the volume of water in a single cell based on fluorescence being inversely proportional to intracellular water concentration. Quantitative imaging of GFP was also used in cultured cells to determine the concentration of GFP and/or its fusion partner (Piston et al., 1999). This inverse relationship is difficult to show in slices or *in vivo*, perhaps because we choose the brightest cells where excess GFP obscures such a relationship. More importantly, volume changes to whole tissue cause poorly defined optical shifts in how excitation and emission photons course through the bulk sample. Nevertheless we measured fluorescence intensity of GFP in astrocytes in control and at 5 min of osmotic challenge. Single optical sections in the same focal plane were used for both conditions. After background subtraction the average fluorescence intensity was measured with ImageJ in the same position over the small soma area in the control and experimental images and the percent change was calculated.

There were technical challenges involved with time-lapse imaging since the volume of the entire slice was dramatically altered during the initial minutes of osmotic challenge, OGD or high K^+ treatment, resulting in the shifting of the focal plane. We therefore sampled single optical sections on the fly, while re-centering and adjusting the field of focus prior to acquiring image stacks (Andrew et al., 2007). In some OGD experiments slice swelling was accompanied by a generally reduced GFP fluorescence, likely involving changes in the optical properties of the tissue but not involving photobleaching or laser damage. Therefore experiments with a faded OGD field were excluded from analysis. Sometimes astrocytes were shifted out of register in two-dimensional space as result of rotation, precluding their analysis.

SigmaStat (Systat, San Jose, CA) was used to compute paired *t*-test and repeated measures analysis of variance (ANOVA) followed by Tukey's *post hoc* method. The significance criterion is set at $P < 0.05$. Data are presented as mean ± SEM. Time is given as mean ± SD.

RESULTS

Astroglial Volume Changes Induced by Acute Osmotic Stress in Brain Slices

Slices with GFP-expressing astrocytes can be imaged in real-time to observe structural changes induced by osmotic stress. Astrocytes included in this study were imaged at a slice depth >50 μm from the cut surface. The majority were deeper than 100 μm where neuropil preservation is optimal (Davies et al., 2007; Kirov et al., 1999). Recently using 2PLSM in slices, we reported preliminary findings of astroglial responses to acute osmotic challenge (Andrew et al., 2007). Here osmotic responses from a total of 56 GFP-expressing astrocytes in 29 slices from 8 animals were analyzed in detail. In all experiments, baseline images were acquired in control ACSF (291–293 mOsm) for 15–20 min.

Eight slices from 3 animals were subjected to hypo-osmotic ACSF and then to hyper-osmotic ACSF, using mannitol, followed by return to control ACSF in a subset of slices (Fig. 1). A steady shift in the focal plane during the first 3 min of osmotic challenge confirmed an overall change in the slice volume. Astrocyte somata superfused with -40 mOsm ACSF for 15 min significantly increased in area as derived from MIP images and then significantly decreased from control following 15 min in +40 mOsm ACSF. Area measurements returned to control following 15 min in normosmotic ACSF (Fig. 1A1—A4). Astroglial swelling and shrinking were also detected when corresponding MIP image stacks acquired in hypo- and hyper-osmotic ACSF were overlaid (Fig. 1A5—A6). This paradigm was repeated in a total of 6 slices. In addition, 2 slices were exposed to either -50/+50 or -60/+60 mOsm ACSF followed by control ACSF.

Compared with control ACSF, mean astroglial area increased significantly by 17.9 ± 2.8% ($P < 0.001$, Fig. 1D1) during 17.7 ± 3 min of overhydration. During 17.1 ± 2.8 min of dehydration, this value decreased to 11.7% ± 1.5% below control ($P < 0.001$, Fig. 1D1) and returned to within 2% ± 2.7% of control ($P = 1.0$, NS from Control) during 15.8 ± 3.6 min of superfusion with normosmotic ACSF (Fig. 1D1). During 15–20 min of osmotic challenge, images were collected in the first few minutes when volume regulation is purported to compensate for osmotic swelling or shrinking (not shown). There was no indication of either RVD during hypo-osmotic challenge or RVI during hyper-osmotic treatment, suggesting that astrocytes passively changed their volume during osmotic challenge without any apparent active volume regulation toward baseline.

To further verify these observations, the order of the osmotic challenges was reversed in 7 slices from 4 animals. Slices were exposed to hyper-osmotic ACSF (+40 or +80 mOsm) and then to hypo-osmotic ACSF (-40 mOsm) followed by control ACSF. Previously we demonstrated that neurons and dendrites steadfastly maintain their volume during acute osmotic stress (Andrew et al., 2007). Figure 1C1—C3 shows a dendrite and astrocyte in hippocampal slice from a hybrid mouse expressing GFP in neurons and astrocytes. While the dendritic volume remained stable, the astroglial soma shrank during 15 min in hyper-osmotic ACSF (Fig. 1C2) and recovered during 15 min in normosmotic ACSF (Fig. 1C3). Relative to control, the mean astroglial soma area significantly decreased by 10.8% ± 1.2% ($P < 0.001$, Fig. 1D2) during 17.2 ± 2.3 min of hyper-osmotic stress, then increased by 9.1% ± 2.4% over control during 17.9 ± 2 min of hypo-osmotic treatment ($P < 0.01$, Fig. 1D2). During re-exposure for 17.4 ± 1.7 min to control ACSF, this value returned to within 4.1% ± 3.3% of baseline ($P = 0.19$, NS from Control, Fig. 1D2). Again these astrocytes showed no apparent volume regulation during the first minutes of osmotic change in this reversed sequence of challenges.

These astroglial responses to osmotic stress were replicated in 3 slices from 2 animals containing astrocytes stained with the astrocyte-specific marker SR101 as shown in Fig. 1B1—B3. Compared with GFP-expressing astrocytes, SR101 lightly stains processes and capillary end-feet but somata are fluorescent enough to measure their MIP area. Relative to control, the mean SR101-labeled astroglia soma area significantly increased by 17.0% ± 4.4% ($P < 0.01$, $n = 4$ astrocytes) during 17.5 ± 1.7 min of exposure to hypo-osmotic ACSF (-40 mOsm) and then decreased by 26.9% ± 9.1% ($P < 0.05$, $n = 4$ astrocytes) during 15.3 ± 3.5 min of hyper-osmotic stress (+40 mOsm). Thus experiments with SR101 confirmed that structural changes observed in GFP-expressing astrocytes were associated with passive volume change, and that the presence of transgene was not altering their osmotic response.

It is possible that astrocytes swell or shrink in the initial 5 min of osmotic challenge and then volume regulate during the next 15 min. Such compensation would not have been detected by sampling at 15–20 min (Fig. 1). Therefore, images were sampled following 5 min of osmotic challenge in 14 slices from 7 animals (Fig. 2). In a subset of experiments, slices from 3 mice

of the enhanced GFP strain were used. Overlaying a soma in control and experimental ACSF at 5 min (Figs. 2A1,B1) revealed cell body swelling in hypo-osmotic ACSF (Fig. 2A2) and shrinking in hyper-osmotic ACSF (Fig. 2B2). Most importantly, astroglial area increased by 12.8% ± 1.1% of control ($P < 0.001$, Fig. 2A3) during 4.9 ± 0.2 min of exposure to -40 mOsm ACSF and decreased by 10.0% ± 1.1% of control ($P < 0.001$, Fig. 2B3) during 4.9 ± 0.1 min of exposure to +40 mOsm ASCF.

As the number of intracellular GFP molecules does not change during osmotic challenge, the fluorescence should be inversely related to the intracellular water concentration (Crowe et al., 1995; Piston et al., 1999). Indeed hyper-osmotic stress resulted in 8.6% ± 3.8% ($P < 0.001$) increase in the soma GFP signal as compared with the control ($n = 19$ astrocytes from 9 slices). Hypo-osmotic challenge resulted in 21.1% ± 7.6% ($P < 0.001$) decrease in the soma GFP signal relative to the control ($n = 18$ astrocytes from 6 slices).

Thus the cohort of cells sampled at 5 min (Fig. 2) display volume increases and decreases similar to cohorts sampled at 15–20 min (Fig. 1). The absence of even a trend toward greater volume change measured at 5 versus 15–20 min indicates that volume changes are near-maximal by 5 min and that active volume regulation is not compensating during the intervening 10–15 min.

Astroglial Swelling Following Depolarization by Elevating $[K^+]_O$

We next used 2PLSM to determine if briefly elevating extracellular potassium would swell astrocytes, in conjunction with their role in the uptake of excess $[K^+]_O$. We exposed CA1 hippocampal astrocytes in 6 slices from 3 animals to 26 mM K^+ ACSF for 3 min (Fig. 3). The image sequence of an astrocyte in control, 26 mM K^+ ACSF and return to control ACSF (wash) is presented in Fig. 3A1—A3. Overlaying MIP images from control and elevated $[K^+]_O$ conditions (Fig. 3A4) as well as during wash (Fig. 3A5) facilitated visual comparison between treatments. Astrocytes swelled as measured at 3.6 ± 0.4 min after the introduction of the 26 mM K^+ ACSF by 38.9% ± 13% ($P < 0.001$, Fig. 3B) and then recovered following a 20 min wash (8.7% ± 9%, $P = 0.35$, NS from Control, Fig. 3B). We conclude that astrocytes swell reversibly in a manner consistent with their ability to buffer excess $[K^+]_O$.

Astroglial Swelling and Partial Recovery Following Simulated Stroke in Slices

The reversibility of both osmotic and K^+-evoked swelling of astrocytes generated confidence that glial responses to stroke-like events could be reliably imaged with 2PLSM. In particular, AD occurs within minutes of stroke onset, causing acute neuronal death (Kaminogo et al., 1998). To clearly delineate the morphological changes that occur within astrocytes following AD, we first used a brain slice model of OGD to simulate global ischemia (Obeidat and Andrew, 1998). Imaging of astrocytes and dendrites revealed swelling of both glial somata and dendritic processes following OGD (Fig. 4A). In addition, swollen dendrites lost their spines and became beaded (Fig. 4A2), a neuronal injury that immediately follows AD both *in vitro* (Andrew et al., 2007; Davies et al., 2007) and *in vivo* (Murphy et al., 2008).

Tissue swelling evoked by OGD for 10 min was accompanied by a progressive shift in the imaging focal plane starting at about 4 min. Ten slices from 6 animals showed a 29.0% ± 6% astroglial area increase from control measurements ($P < 0.001$, Fig. 4E). Similar increases in soma size of SR101-labeled astrocytes confirmed a volume increase not confined to GFP-expressing astrocytes (Fig. 4B). Neuronal cell bodies simultaneously swelled during OGD (Figs. 4B and 5B) as previously quantified (Andrew et al., 2007).

Having confirmed real-time astroglial swelling in response to OGD, we looked at its time-course in more detail. Using 9 slices from 5 animals, we acquired images of single optical

sections of 12 GFP-expressing astrocytes to derive a time-course for soma swelling during 10 min of OGD (Fig. 4C). Images were taken once every minute for 10 min. Astrocytes started to swell at 5 min (Fig. 4C4) (10.7% ± 4%, $P < 0.01$, Fig. 4F) and remained swollen for the entire 10 min period (Figs. 4C6,F) (10.6% ± 3%; $P < 0.05$, Fig. 4F). Using a similar sequence taken from hybrid mice, we were able to compare the time-course of astroglial swelling with that of dendrites (Fig. 4D). The dendritic response to OGD followed the astroglial response closely (Fig. 4D4). These findings suggest that glial and neuronal swelling reliably occur in the first few minutes following OGD *in vitro*.

We next used 2PLSM to determine the extent of astroglial and neuronal recovery from ischemia. Ten minutes of OGD reliably induced cell swelling, so we introduced a post-OGD period of re-oxygenation/normoglycemia, using control ACSF, and recorded the changes in soma area during this recovery period (Fig. 5). Nine slices from 5 animals showed that astroglial soma area significantly increased during 10 min of OGD (20.0% ± 13%, $P < 0.01$, Figs. 5A2,C1) but rapidly returned to near baseline within 1 min of re-exposure to control ACSF (-0.5% ± 6%; $P = 0.12$, NS from Control, Figs. 5A3,C1). Seven slices from 6 animals showed neuronal soma swelling by 30.5% ± 19% during OGD ($P < 0.001$, Figs. 5B2,C2) but no recovery during re-oxygenation (35.5% ± 19%, $P < 0.001$, Figs. 5B3,C2). We conclude that although astrocytes and neurons swell similarly in response to global ischemia in slices, only astrocytes have the ability to recover morphologically to some degree.

Astroglial Swelling Observed *in vivo*

After monitoring astroglial volume changes in slices, we then used noninvasive *in vivo* imaging to examine changes in native astrocytes concurrently with changes in blood flow. Cranial windows allowed visualization of blood vessels and GFP-expressing astrocytes within living mice. We first wanted to confirm that the osmotic stress-induced swelling seen in slices could be observed *in vivo*. Astrocytes were imaged in layer II/III of somato-sensory cortex at a depth of about 100 μm (Figs. 6A,B). Hypo-osmotic stress was induced by IP distilled water injection (150 mL/kg). 2PLSM images obtained from 10 animals revealed rapid astroglial soma swelling during the initial 6 min following water injection (Fig. 6C). Soma area increased by 9.7% ± 10% ($P < 0.05$, Fig. 6C) at 3.0 ± 0.3 min and by 21.1% ± 13% ($P < 0.001$, Fig. 6C) at 9.5 ± 0.3 min (Figs. 6A2,B2). The increased soma size persisted throughout the 12–30 min period following water injection ($P < 0.001$, Fig. 6C), emphasizing a lack of RVD *in vivo*, confirming our slice findings.

Out of the 21 astrocytes included in this analysis, only 4 fell into the category of "perivascular astrocytes;" i.e., an astrocyte whose soma directly contacted a blood vessel (Fig. 6A1). The remaining 17 astrocytes contacted blood vessels via processes/end-feet. During our imaging of layers II/III of somatosensory cortex, we observed that all astrocytes contacted at least one blood vessel via their soma or a process. The rapid soma swelling observed in this study was not restricted to perivascular astrocytes (Fig. 6A1,A2, and Supp. Info. Fig. 2), but also occurred in those with the soma distant from the blood vessel (Fig. 6B1,B2, and Supp. Info. Fig. 2).

As astroglial responses to osmotic stress *in vivo* nicely correlated with those in slices, we next examined if astrocytes would react to ischemic stress in the same manner. As shown in Fig. 4, AD induced by OGD resulted in astroglial soma swelling within 5 min *in vitro*. In our *in vivo* model, CA induced global ischemia, likely causing AD of neurons and glia within 1–3 min (although onset was not measured) (Chuquet et al., 2007;Murphy et al., 2008). Images obtained before CA (>50 μm deep in layer II/III of somatosensory cortex) were used as controls with subsequent images acquired at varying times after CA (Fig. 7). We were able to confirm CA by monitoring heart rate and visually by the loss of "streaking" in vessels (representing flow of nonfluorescent red blood cells) (Fig. 7A1,A2). In 6 animals imaged at 8.9 ± 0.6 min following CA, somata swelled similarly to the glial response to global ischemia in slices (Fig.

7A) (33.3% ± 8%, $P < 0.01$, Fig. 7B1). Astroglial processes also swelled (Fig. 7A), although these changes were not quantifiable because of the resolution limitations and brightness of GFP signal. However, the arbor that defines an astroglial domain (Bushong et al., 2002) did not change in size despite obvious swelling in the processes themselves (Fig. 7A) (3.2% ± 4%; $P = 0.808$, NS from Control, Fig. 7B2). Thus, astroglial swelling induced by global ischemia *in vivo* provided similar results to ischemia in slices, supporting our *in vitro* experiments.

DISCUSSION

We used real-time imaging to directly examine osmotic- and ischemia-induced volume change in astrocytes. Our findings are similar both in brain slices and *in vivo* as imaged through cranial window preparations. Astrocytes and their processes swell or shrink passively in response to osmotic challenge and swell during ischemia. As seen in slices, volume recovery begins immediately upon the resupply of O_2/glucose. We did not detect any evidence for acute volume regulation by astrocytes throughout the osmotic or ischemic challenges, despite cell volume sampling at each minute during and following a challenge. The concept of RVD is predicated on the observation that strong osmotic change first alters volume and then volume regulation occurs. In this regard, we never observed a volume decrease during osmotic challenge over many minutes once an astrocyte swelled. Chvátal et al. (2007) reported only slight RVD in a few astrocytic somata in slices at room temperature and even this required a 100 mOsm dilution.

Passive Volume Changes in Astrocytes in Cortical Slices During Osmotic Challenge

Pyramidal neurons in cortical slices maintain their volume during osmotic stress (Andrew et al., 2007). In the present study, neocortical and hippocampal astrocytes alter their volume in response to osmotic challenge. This ability is likely because astrocytes express abundant water-selective aquaporins (Amiry-Moghaddam and Ottersen, 2003; Nielsen et al., 1997), whereas pyramidal neurons have not been reported to express functional aquaporins in their plasma membrane. Simultaneous 2PLSM imaging confirmed the osmosensitivity of astroglial cells and the osmoresistant quality of neurons.

In cell culture or in dissociated preparations, astrocytes are reported to not only change their volume in response to strong osmotic stress, but to also then regulate their volume over a period ranging from seconds to minutes (Olson et al., 1995; Ordaz et al., 2004). *in vivo*, osmotic volume regulation develops over many hours and days (see Introduction) but there is no evidence to date that it is evoked over seconds to minutes in the intact brain. Cserr et al. (1991) reported that brain cell volume was unchanged 30 min after an IP injection of NaCl that raised plasma osmolality to ~ 360 mOsm in the rat. However at 15 min, the Na^+ was just entering the brain's extracellular fluid (their Fig. 6) so whether RVI occurs over the first 30 min is unknown. As Cserr et al. noted, RVI has been rarely reported in isolated brain cells. In brain slices, RVD has been reported under high hypo-osmotic stress (Kreisman and Olson, 2003) but this was also observed in slices considered damaged by that stress (Andrew et al., 1997). If neurons are indeed osmoresistant (Andrew et al., 2007) then volume regulation in slices should be driven by astrocytes. Our previous work revealed no evidence of RVD in cortical slices based on measurements of both changes in tissue light transmittance and extracellular resistance (Andrew et al., 1997, 2007; Andrew and MacVicar, 1994). Here, experiments using a 5 min exposure to hypo- or hyper-osmotic ACSF produced passive astroglial responses similar to longer-duration (15–20 min) challenges. Pre-incubation of some slices with 1 mM taurine, proposed to promote volume regulation, was not effective in evoking either RVD or RVI. In accordance with our results no astroglial RVD was observed in hippocampal slices under high hypo-osmotic stress at room temperature (Hirrlinger et al., 2008). Our findings indicate that astrocytes do not undergo active volume compensation after the initial period of swelling or shrinking under physiologically relevant osmotic conditions

and temperature. Rather, the volume changes are easily explained by water passively flowing down an imposed osmotic gradient, conducted by aquaporins abundant in the plasma membranes of both endothelia (Grande et al., 1997) and astroglia (Badaut et al., 2004; Solenov et al., 2004).

In most experiments we examined changes in somatic area of astrocytes as reflecting their relative change in volume, which we assume is more or less equal in all dimensions (see Materials and Methods). Change in a preferred direction is possible but unprecedented. The likelihood that astroglial soma size increased in the *x*—*y* plane, while decreasing in z-dimension (with the consequence that RVD was systemically undetected) seems unlikely. In addition, a 5 min osmotic challenge revealed increased soma GFP fluorescence during dehydration and decreased fluorescence during over-hydration, further arguing that we did not miss active volume regulation in our MIP images.

Astroglial Dynamics in Cortical Slices Following Depolarization

Astrocytes play a critical role in the buffering of potassium from extracellular space (Kofuji and Newman, 2004). Elevated $[K^+]_O$ levels lead to reversible membrane depolarization of astrocytes, accumulation of $[K^+]_I$ and water intake through aquaporins (Binder et al., 2006; Manley et al., 2004; Walz, 1997). Real-time 2PLSM imaging shows that increased $[K^+]_O$ reliably and reversibly swells astroglial somata. Elevated $[K^+]_O$ is linked to depolarizations during stroke (Leis et al., 2005; Vorisek and Sykova, 1997; Xie et al., 2007) and the electroneutral uptake of K^+ and Cl^- by astrocytes contributes to brain edema (Mongin and Kimelberg, 2004). We report here that OGD-induced AD immediately leads to profound astroglial swelling in cortical slices, as is the case with K^+-induced depolarization.

Electrophysiological studies in hippocampal slices show that astrocytes display some recovery from OGD-induced depolarization, whereas neurons do not (Xie et al., 2007). Our 2PLSM imaging in slices reveals that astrocytes not only swell in response to OGD-evoked AD but recover within minutes of re-oxygenation/normoglycemia. These changes occur at a much faster time-course than reported in cell culture studies showing aquaporin-facilitated swelling and recovery of astrocytes over several days (Fu et al., 2007). At the same time, swollen neurons display no recovery of form in our experiments. The rapid recovery of astrocytes from transient ischemic stress helps account for astroglial survival *in vivo* in the ischemic core while adjacent neurons die (Pekny and Nilsson, 2005). We propose that neurons may be less likely to recover because their plasma membrane is aquaporin-deficient. However, beaded dendrites can recover normal morphology during reperfusion *in vivo* after brief focal stroke or transient global ischemia (Murphy et al., 2008; Zhang et al., 2005). It is likely then that if energy stores quickly recover, water can be shunted from neurons, possibly by the *N*-acetyl aspartic acid (NAA) molecular water pump (Baslow et al., 2007). Also in hippocampal slices, dendrites rapidly recover from cold-induced beading when energy stores become accessible with warmer temperatures (Kirov et al., 2004). However in slices at 33°C, 10 min of OGD severely compromises neuronal energy sources and, without a route for passive water efflux through aquaporins, we argue that neurons remain swollen and their dendrites beaded.

Tracking Astroglial Changes *in vivo*

Our slice findings prompted the question: Can these rapid astroglial volume responses be observed *in vivo*? Previous experiments that induced hypo-osmotic conditions in cerebellar cortex of live rats demonstrated histological evidence for volume regulation following 4 h of IP injection of distilled water (Nagelhus et al., 1993,1996). Using this technique, we have shown that astrocytes swell within minutes of the injection, as imaged by 2PLSM through an open-glass cranial window. Attempts to track recovery upon return to baseline osmolality (using hypertonic saline injection) were unsuccessful, the result of a general dimming of GFP

as the optical properties of the swollen tissue changed. Nevertheless, this paradigm did replicate the rapid astroglial soma swelling that we observed in slices. Also, no RVD was detected during the initial 30 min. Recently Nase et al. (2008) utilized a thinned skull window and IP water injection to show that astrocytes in close proximity to blood vessels slowly swelled over 2 h whereas astrocytes away from vessels either maintained or decreased their size (their Fig. 4). This is at odds with astrocytes forming a tight syncytium linked by water permeable gap junctions. In all our experiments with an open-glass (Fig. 6) or a thinned skull (Supp. Info. Fig. 2) cranial window (Grutzendler and Gan, 2005), we observed a rapid change in astroglial size independent of their proximity to blood vessels. Water traverses brain capillaries through aquaporins, entering interstitial space and then perivascular end-feet (Nase et al., 2008) resulting in a quick rise of intracranial pressure (Yang et al., 2008). But an astrocyte should also quickly take up water through aquaporins located on its soma and processes as well as from neighbors linked by gap junctions, even without the soma directly apposed to a blood vessel. Our data support that scenario.

We used CA as an *in vivo* model of global ischemia. Cessation of blood flow quickly evokes AD in intact mice (Murphy et al., 2008), similar to OGD in cortical slices (Joshi and Andrew, 2001). Here, we observed a rapid swelling of astrocyte somata and processes similar to our slices during OGD exposure. The CA model does not permit study of reperfusion *in vivo* so astrocyte recovery during reperfusion is the subject of future studies.

The astroglial component of brain swelling at stroke onset is thought to be primarily mediated by aquaporin 4 (AQP4) (Amiry-Moghaddam and Ottersen, 2003; Rash et al., 1998). In the human brain, increased astroglial AQP4 protein levels were found at the periphery of ischemic foci suggesting that post-ischemic upregulation of AQP4 might exacerbate brain edema (Aoki et al., 2003). Accordingly, slower dissipation of brain edema after stroke may result from reduction of AQP4 in perivascular astrocyte end-feet in mice (Amiry-Moghaddam et al., 2003).

Astrocytes typically form distinct boundaries that define their region of influence in the mature brain (Bushong et al., 2002,2004;Ogata and Kosaka, 2002). Although astroglial processes swelled following AD *in vivo*, the extent of arborization remained unchanged. This finding is in accordance with a previous study showing process swelling without expansion of the astroglial domain following stroke and other conditions of brain injury (Wilhelmsson et al., 2006).

CONCLUSIONS

Based on the findings presented here and our previous work (Andrew et al., 1997,2007), we propose that the brain's neuronal compartment is, for the most part, osmotically water-tight and so volume regulation over the seconds and minutes following acute osmotic challenge is unnecessary for neurons. Over this same brief time frame, astrocytes exposed to survivable levels of osmotic stress passively change volume, requiring tens of minutes to begin volume regulating at levels detectable *in vivo* (Cserr et al., 1991;Krizaj et al., 1996; Nagelhus et al., 1993,1996). The pathway by which water enters neurons upon AD is not yet known. The concept that during depolarization, Na^+ and Cl^- influx draws water into neurons and so swells the cell is popular but both ions are almost completely stripped of their hydration shells as they transit their channels (MacAulay et al., 2004). Water will not rapidly follow without aquaporins spanning the plasma membrane. One possibility is that during ischemia, unpaired gap junctions (or another large-pore channel) open (Anderson et al., 2005;Spray et al., 2006;Thompson et al., 2006). However as water builds up in neurons, their lack of aquaporins means that the hydrostatic pressure cannot be relieved by the loss of water unless oxygen and glucose levels are quickly restored. Astrocytes, in contrast, have no such impediment.

Supplementary Material

Refer to Web version on PubMed Central for supplementary material.

ACKNOWLEDGMENTS

The authors thank Dr. H. Kettenmann (Max Delbruck Center for Molecular Medicine, Berlin, Germany) for his generous gift of (GFAP-EGFP) transgenic mice and Dr. J. Sanes (Harvard University, Boston, MA, USA) for his generous gift of (GFP-M) transgenic mice. The authors thank members of Dr. Kirov's laboratory Ms. Deborah Ard and Dr. Jianghe Yuan for their excellent technical assistance.

Grant sponsor: National Institutes of Health; Grant number: RO1 NS057113; Grant sponsor: Heart and Stroke Foundation (Ontario); Grant number: T-4478; Grant sponsor: Canadian Institutes of Health Research; Grant number: MOP69044.

REFERENCES

Amiry-Moghaddam M, Otsuka T, Hurn PD, Traystman RJ, Haug FM, Froehner SC, Adams ME, Neely JD, Agre P, Ottersen OP, Bhardwaj A. An a-syntrophin-dependent pool of AQP4 in astroglial end-feet confers bidirectional water flow between blood and brain. Proc Natl Acad Sci USA 2003;100:2106–2111. [PubMed: 12578959]

Amiry-Moghaddam M, Ottersen OP. The molecular basis of water transport in the brain. Nat Rev Neurosci 2003;4:991–1001. [PubMed: 14682361]

Anderson TR, Jarvis CR, Biedermann AJ, Molnar C, Andrew RD. Blocking the anoxic depolarization protects without functional compromise following simulated stroke in cortical brain slices. J Neurophysiol 2005;93:963–979. [PubMed: 15456803]

Andrew RD. Seizure and acute osmotic change: Clinical and neurophysiological aspects. J Neurol Sci 1991;101:7–18. [PubMed: 2027029]

Andrew RD, Labron MW, Boehnke SE, Carnduff L, Kirov SA. Physiological evidence that pyramidal neurons lack functional water channels. Cereb Cortex 2007;17:787–802. [PubMed: 16723408]

Andrew RD, Lobinowich ME, Osehobo EP. Evidence against volume regulation by cortical brain cells during acute osmotic stress. Exp Neurol 1997;143:300–312. [PubMed: 9056392]

Andrew RD, MacVicar BA. Imaging cell volume changes and neuronal excitation in the hippocampal slice. Neuroscience 1994;62:371–383. [PubMed: 7830884]

Aoki K, Uchihara T, Tsuchiya K, Nakamura A, Ikeda K, Wakayama Y. Enhanced expression of aquaporin 4 in human brain with infarction. Acta Neuropathol (Berl) 2003;106:121–124. [PubMed: 12715185]

Badaut J, Petit JM, Brunet JF, Magistretti PJ, Charriaut-Marlangue C, Regli L. Distribution of Aquaporin 9 in the adult rat brain: Preferential expression in catecholaminergic neurons and in glial cells. Neuroscience 2004;128:27–38. [PubMed: 15450351]

Baslow MH, Hrabe J, Guilfoyle DN. Dynamic relationship between neurostimulation and *N*-acetylaspartate metabolism in the human visual cortex: Evidence that NAA functions as a molecular water pump during visual stimulation. J Mol Neurosci 2007;32:235–245. [PubMed: 17873369]

Binder DK, Yao X, Zador Z, Sick TJ, Verkman AS, Manley GT. Increased seizure duration and slowed potassium kinetics in mice lacking aquaporin-4 water channels. Glia 2006;53:631–636. [PubMed: 16470808]

Bushong EA, Martone ME, Ellisman MH. Maturation of astrocyte morphology and the establishment of astrocyte domains during post-natal hippocampal development. Int J Dev Neurosci 2004;22:73–86. [PubMed: 15036382]

Bushong EA, Martone ME, Jones YZ, Ellisman MH. Protoplasmic astrocytes in CA1 stratum radiatum occupy separate anatomical domains. J Neurosci 2002;22:183–192. [PubMed: 11756501]

Chan PH, Fishman RA. Elevation of rat brain amino acids, ammonia and idiogenic osmoles induced by hyperosmolality. Brain Res 1979;161:293–301. [PubMed: 758976]

Chuquet J, Hollender L, Nimchinsky EA. High-resolution in vivo imaging of the neurovascular unit during spreading depression. J Neurosci 2007;27:4036–4044. [PubMed: 17428981]

Chvátal A, Andrová M, Kirchhoff. Three-dimensional confocal morphometry—A new approach for studying dynamic changes in cell morphology in brain slices. J Anat 2007;210:671–683. [PubMed: 17488344]

Crowe WE, Altamirano J, Huerto L, Alvarez-Leefmans FJ. Volume changes in single N1E-115 neuroblastoma cells measured with a fluorescent probe. Neuroscience 1995;69:283–296. [PubMed: 8637626]

Cserr HF, DePasquale M, Nicholson C, Patlak CS, Pettigrew KD, Rice ME. Extracellular volume decreases while cell volume is maintained by ion uptake in rat brain during acute hypernatremia. J Physiol 1991;442:277–295. [PubMed: 1798030]

Davies ML, Kirov SA, Andrew RD. Whole isolated neocortical and hippocampal preparations and their use in imaging studies. J Neurosci Methods 2007;166:203–216. [PubMed: 17765319]

Feng G, Mellor RH, Bernstein M, Keller-Peck C, Nguyen QT, Wallace M, Nerbonne JM, Lichtman JW, Sanes JR. Imaging neuronal subsets in transgenic mice expressing multiple spectral variants of GFP. Neuron 2000;28:41–51. [PubMed: 11086982]

Finberg L. Appropriate therapy can prevent cerebral swelling in diabetic ketoacidosis. J Clin Endocrinol Metab 2000;85:508–509.

Fishman RA. Brain edema. N Engl J Med 1975;293:706–711. [PubMed: 1160939]

Fried HU, Linnig HD, Korsching SI. An inexpensive mouse head-holder suitable for optical recordings. Physiol Behav 2001;74:253–255. [PubMed: 11714486]

Fu X, Li Q, Feng Z, Mu D. The roles of aquaporin-4 in brain edema following neonatal hypoxia ischemia and re-oxygenation in a cultured rat astrocyte model. Glia 2007;55:935–941. [PubMed: 17437301]

Grande PO, Asgeirsson B, Nordstrom CH. Physiologic principles for volume regulation of a tissue enclosed in a rigid shell with application to the injured brain. J Trauma 1997;42:S23–S31. [PubMed: 9191692]

Grutzendler, J.; Gan, WB. A practical guide: Long-term two-photon transcranial imaging of synaptic structures in the living brain. In: Yuste, R.; Konnerth, A., editors. Imaging in neuroscience and development: A laboratory manual. Cold spring Harbor Laboratory Press; Cold Spring Harbor: 2005. p. 185-189.

Gullans SR, Verbalis JG. Control of brain volume during hyperosmolar and hypoosmolar conditions. Annu Rev Med 1993;44:289–301. [PubMed: 8476251]

Hirrlinger PG, Wurm A, Hirrlinger J, Bringmann A, Reichenbach A. Osmotic swelling characteristics of glial cells in the murine hippocampus, cerebellum, and retina in situ. J Neurochem 2008;105:1405–1417. [PubMed: 18221375]

Holtmaat, AJ.; Wilbrecht, L.; Karpova, A.; Portera-Cailliau, C.; Burbach, B.; Trachtenberg, T.; Svoboda, K. Long-term, high-resolution imaging of neurons in the neocortex in vivo. In: Yuste, R.; Konnerth, A., editors. Imaging in neuroscience and development: A laboratory manual. Cold spring Harbor Laboratory Press; Cold Spring Harbor: 2005. p. 627-638.

Joshi I, Andrew RD. Imaging anoxic depolarization during ischemia-like conditions in the mouse hemi-brain slice. J Neurophysiol 2001;85:414–424. [PubMed: 11152742]

Kaminogo M, Suyama K, Ichikura A, Onizuka M, Shibata S. Anoxic depolarization determines ischemic brain injury. Neurol Res 1998;20:343–348. [PubMed: 9618699]

Kimelberg HK. Water homeostasis in the brain: Basic concepts. Neuroscience 2004;129:851–860. [PubMed: 15561403]

Kirov SA, Petrak LJ, Fiala JC, Harris KM. Dendritic spines disappear with chilling but proliferate excessively upon rewarming of mature hippocampus. Neurosci 2004;127:69–80.

Kirov SA, Sorra KE, Harris KM. Slices have more synapses than perfusion-fixed hippocampus from both young and mature rats. J Neurosci 1999;19:2876–2886. [PubMed: 10191305]

Kofuji P, Newman EA. Potassium buffering in the central nervous system. Neuroscience 2004;129:1045–1056. [PubMed: 15561419]

Kreisman NR, Olson JE. Taurine enhances volume regulation in hippocampal slices swollen osmotically. Neuroscience 2003;120:635–642. [PubMed: 12895504]

Krizaj D, Rice ME, Wardle RA, Nicholson C. Water compartmentalization and extracellular tortuosity after osmotic changes in cerebellum of Trachemys scripta. J Physiol 1996;492(Part 3):887–896. [PubMed: 8734998]

Leis JA, Bekar LK, Walz W. Potassium homeostasis in the ischemic brain. Glia 2005;50:407–416. [PubMed: 15846795]

MacAulay N, Hamann S, Zeuthen T. Water transport in the brain: Role of cotransporters. Neuroscience 2004;129:1031–1044. [PubMed: 15561418]

Manley GT, Binder DK, Papadopoulos MC, Verkman AS. New insights into water transport and edema in the central nervous system from phenotype analysis of aquaporin-4 null mice. Neurosci 2004;129:983–991.

Mongin, AA.; Kimelberg, HK. Astrocytic swelling in neuropathology. In: Kettenmann, HO.; Ransom, BR., editors. Neuroglia. Oxford University Press; New York: 2004. p. 550-562.

Murphy TH, Li P, Betts K, Liu R. Two-photon imaging of stroke onset in vivo reveals that NMDA-receptor independent ischemic depolarization is the major cause of rapid reversible damage to dendrites and spines. J Neurosci 2008;28:1756–1772. [PubMed: 18272696]

Nagelhus EA, Lehmann A, Ottersen OP. Neuronal-glial exchange of taurine during hypo-osmotic stress: A combined immunocytochemical and biochemical analysis in rat cerebellar cortex. Neuroscience 1993;54:615–631. [PubMed: 8332252]

Nagelhus EA, Lehmann A, Ottersen OP. Neuronal and glial handling of glutamate and glutamine during hypoosmotic stress: A biochemical and quantitative immunocytochemical analysis using the rat cerebellum as a model. Neuroscience 1996;72:743–755. [PubMed: 9157320]

Nase G, Helm PJ, Enger R, Ottersen OP. Water entry into astrocytes during brain edema formation. Glia 2008;56:895–902. [PubMed: 18351631]

Nielsen S, Nagelhus EA, Amiry-Moghaddam M, Bourque C, Agre P, Ottersen OP. Specialized membrane domains for water transport in glial cells: High-resolution immunogold cytochemistry of aqua-porin-4 in rat brain. J Neurosci 1997;17:171–180. [PubMed: 8987746]

Nimmerjahn A, Kirchhoff F, Kerr JN, Helmchen F. Sulforhodamine 101 as a specific marker of astroglia in the neocortex in vivo. Nat Methods 2004;1:31–37. [PubMed: 15782150]

Nolte C, Matyash M, Pivneva T, Schipke CG, Ohlemeyer C, Hanisch UK, Kirchhoff F, Kettenmann H. GFAP promoter-controlled EGFP-expressing transgenic mice: A tool to visualize astrocytes and astrogliosis in living brain tissue. Glia 2001;33:72–86. [PubMed: 11169793]

Obeidat AS, Andrew RD. Spreading depression determines acute cellular damage in the hippocampal slice during oxygen/glucose deprivation. Eur J Neurosci 1998;10:3451–3461. [PubMed: 9824458]

Ogata K, Kosaka T. Structural and quantitative analysis of astrocytes in the mouse hippocampus. Neuroscience 2002;113:221–233. [PubMed: 12123700]

Olson JE, Alexander C, Feller DA, Clayman ML, Ramnath EM. Hypoosmotic volume regulation of astrocytes in elevated extracellular potassium. J Neurosci Res 1995;40:333–342. [PubMed: 7745627]

Ordaz B, Tuz K, Ochoa LD, Lezama R, Pena-Segura C, Franco R. Osmolytes and mechanisms involved in regulatory volume decrease under conditions of sudden or gradual osmolarity decrease. Neurochem Res 2004;29:65–72. [PubMed: 14992264]

Pekny M, Nilsson M. Astrocyte activation and reactive gliosis. Glia 2005;50:427–434. [PubMed: 15846805]

Piston DW, Patterson GH, Knobel SM. Quantitative imaging of the green fluorescent protein (GFP). Methods Cell Biol 1999;58:31–48. [PubMed: 9891373]

Pollock AS, Arieff AI. Abnormalities of cell volume regulation and their functional consequences. Am J Physiol 1980;239:F195–F205. [PubMed: 7435558]

Rash JE, Yasumura T, Hudson CS, Agre P, Nielsen S. Direct immunogold labeling of aquaporin-4 in square arrays of astrocyte and ependymocyte plasma membranes in rat brain and spinal cord. Proc Natl Acad Sci USA 1998;95:11981–11986. [PubMed: 9751776]

Rosen AS, Andrew RD. Osmotic effects upon excitability in rat neocortical slices. Neuroscience 1990;38:579–590. [PubMed: 2270133]

Solenov E, Watanabe H, Manley GT, Verkman AS. Sevenfold-reduced osmotic water permeability in primary astrocyte cultures from AQP-4-deficient mice, measured by a fluorescence quenching method. Am J Physiol Cell Physiol 2004;286:C426–C432. [PubMed: 14576087]

Spray DC, Ye ZC, Ransom BR. Functional connexin “hemi-channels”: A critical appraisal. Glia 2006;54:758–773. [PubMed: 17006904]

Thompson RJ, Zhou N, MacVicar BA. Ischemia opens neuronal gap junction hemichannels. Science 2006;312:924–927. [PubMed: 16690868]

Traynelis SF, Dingledine R. Role of extracellular space in hyper-osmotic suppression of potassium-induced electrographic seizures. J Neurophysiol 1989;61:927–938. [PubMed: 2723735]

Vorisek I, Sykova E. Ischemia-induced changes in the extra-cellular space diffusion parameters, K+, and pH in the developing rat cortex and corpus callosum. J Cereb Blood Flow Metab 1997;17:191–203. [PubMed: 9040499]

Walz W. Role of astrocytes in the spreading depression signal between ischemic core and penumbra. Neurosci Biobehav Rev 1997;21:135–142. [PubMed: 9062936]

Wilhelmsson U, Bushong EA, Price DL, Smarr BL, Phung V, Terada M, Ellisman MH, Pekny M. Redefining the concept of reactive astrocytes as cells that remain within their unique domains upon reaction to injury. Proc Natl Acad Sci USA 2006;103:17513–17518. [PubMed: 17090684]

Xie M, Wang W, Kimelberg HK, Zhou M. Oxygen and glucose deprivation-induced changes in astrocyte membrane potential and their underlying mechanisms in acute rat hippocampal slices. J Cereb Blood Flow Metab 2007;28:456–467. [PubMed: 17713462]

Yang B, Zador Z, Verkman AS. Glial cell aquaporin-4 overexpression in transgenic mice accelerates cytotoxic brain swelling. J Biol Chem 2008;283:15280–15286. [PubMed: 18375385]

Zhang S, Boyd J, Delaney K, Murphy TH. Rapid reversible changes in dendritic spine structure in vivo gated by the degree of ischemia. J Neurosci 2005;25:5333–5338. [PubMed: 15930381]

Zhuo L, Sun B, Zhang CL, Fine A, Chiu SY, Messing A. Live astrocytes visualized by green fluorescent protein in transgenic mice. Dev Biol 1997;187:36–42. [PubMed: 9224672]

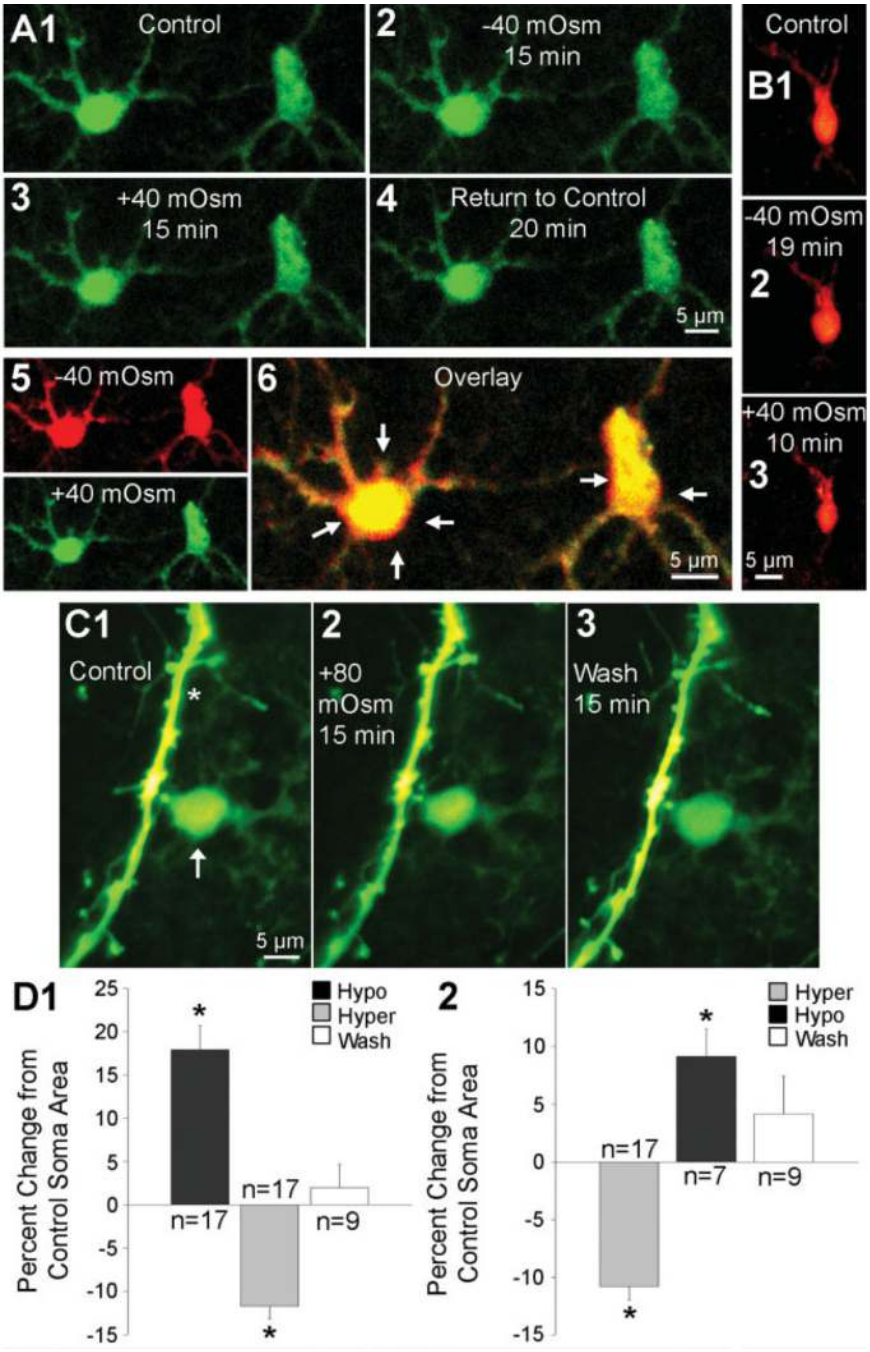

Fig. 1.

2PLSM observation of astrocytes provides no indication of active volume regulation during acute osmotic challenge. **A1**—**A4**: 2PLSM sequence of GFP-expressing astrocytes from CA1 in hippocampal slice. Astrocytes (A1, control) swell during a 15 min superfusion with hypo-osmotic ACSF (A2), shrink during a 15-min treatment with hyper-osmotic ACSF (A3), and then return to baseline volume during 20 min in control ACSF (A4). Hypo-osmotic (**A5**; red) and hyper-osmotic (green) images are overlaid (**A6**) with arrows pointing to red areas illustrating volume differences under these conditions. **B1**—**B3**: 2PLSM sequence of an astrocyte labeled with astrocyte-specific dye SR101. The astrocyte (B1, control) swells under acutely overhydrated conditions (B2) and shrinks when dehydrated (B3). **C1**—**C3**: 2PLSM

sequence of a GFP-expressing astrocyte and dendrite from CA1 in hippocampal slice. The astrocyte (arrow), seen in control in C1, shrinks under hyper-osmotic stress (C2) and recovers in normosmotic ACSF (C3). The dendrite (asterisk), however, is unchanged. **D1**: Quantification of astroglial soma area changes from control to hypo-osmotic to hyper-osmotic conditions and then during return to control ACSF. The number of astrocytes analyzed in 8 slices from 3 animals is indicated for each condition. No active volume regulation was detected. Values are shown as percent change from control. Asterisks indicate significant difference from control (*$P < 0.001$). **D2**: Summary of measurements in 7 slices of 4 animals shifting from control to hyper-osmotic to hypo-osmotic conditions and then returning to control ACSF (*$P < 0.01$). No active volume regulation was detected. Values are shown as percent change from control. Asterisks indicate significant difference from control (*$P < 0.01$).

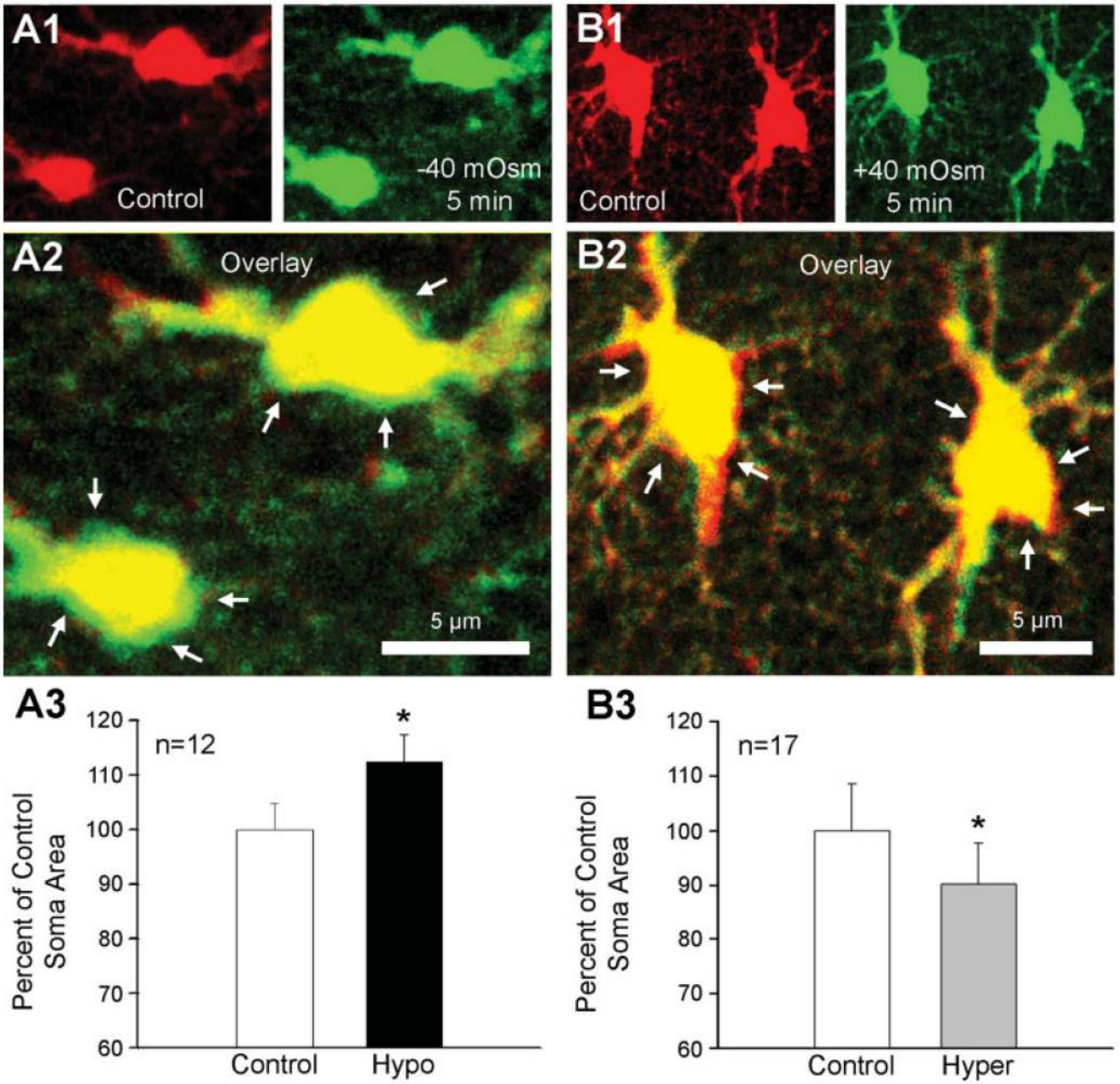

Fig. 2.

Acute osmotic challenge results in a rapid and passive astroglial response. **A1,B1**: 2PLSM images of GFP-expressing astrocytes from CA1 region in hippocampal slice during 5 min of hypo-osmotic (A1) and hyper-osmotic (B1) stress. **A2,B2**: Overlays showing the merged control (red) and experimental (green) images, with arrows pointing at green areas representing swelling during exposure to hypo-osmotic ACSF (A2) or at red areas representing shrinking during exposure to hyper-osmotic ACSF (B2). **A3**: Summary from 12 astrocytes in 6 slices from 6 animals showing no detectable active RVD following soma swelling in response to 5 min of hypo-osmotic stress. Values are shown as percent of control. Asterisk indicates significant difference from control (*$P < 0.001$). **B3**: Summary from 17 astrocytes in 8 slices from 5 animals showing no detectable RVI following soma shrinking in response to 5 min of

hyper-osmotic stress. Values are shown as percent of control. Asterisk indicates significant difference from control (*$P < 0.001$).

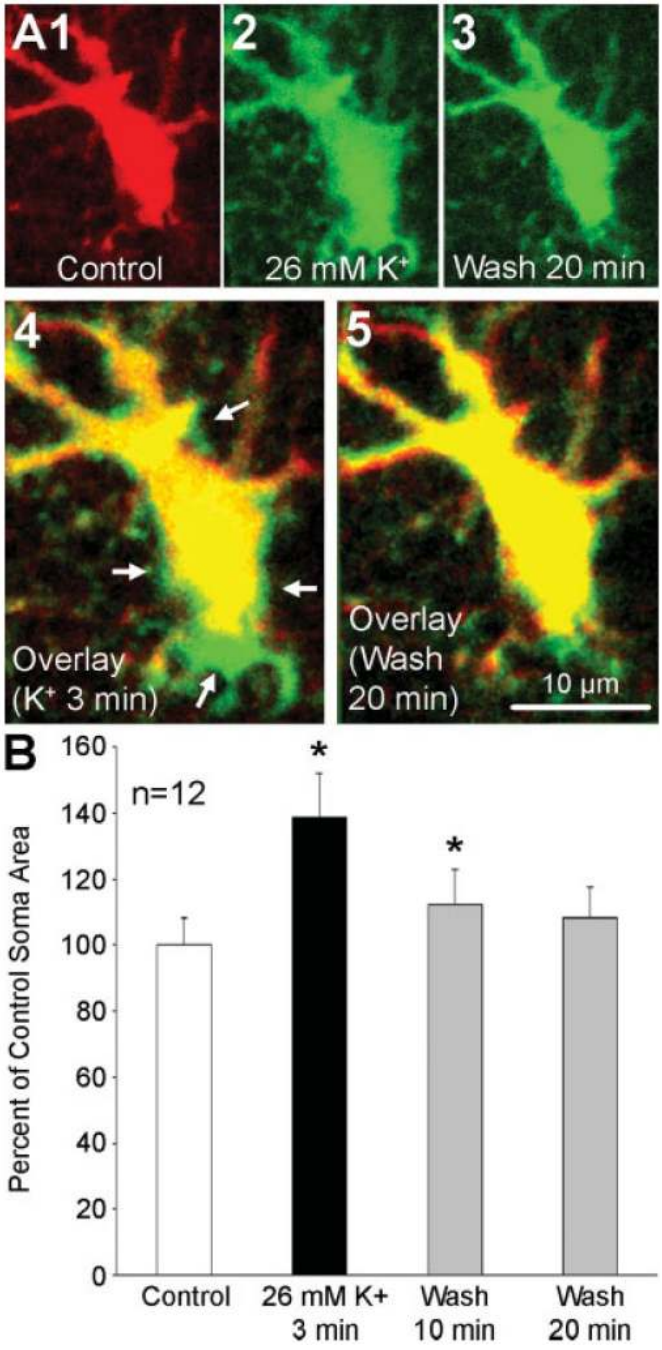

Fig. 3.

Astrocytes swell during high-K^+ treatment and recover in control ACSF. **A1—A3**: 2PLSM sequence of a GFP-expressing astrocyte from CA1 region. The astroglial soma and processes (A1, control) swell during 3 min of exposure to 26 mM K^+ ACSF (A2) and return to control morphology after 20 min in control ACSF (A3). **A4**: Overlay showing the merged control (A1, red) and experimental (A2, green) images. Arrows point to green areas representing swelling during exposure to high K^+ ACSF, which then reverses (**A5**). **B**: Summary from 12 astrocytes in 6 slices from 3 animals showing astroglial soma swelling induced by 3 min exposure to 26 mM K^+ ACSF. Values are shown as percent of control measurements. Asterisks indicate significant difference from control ($*P < 0.001$).

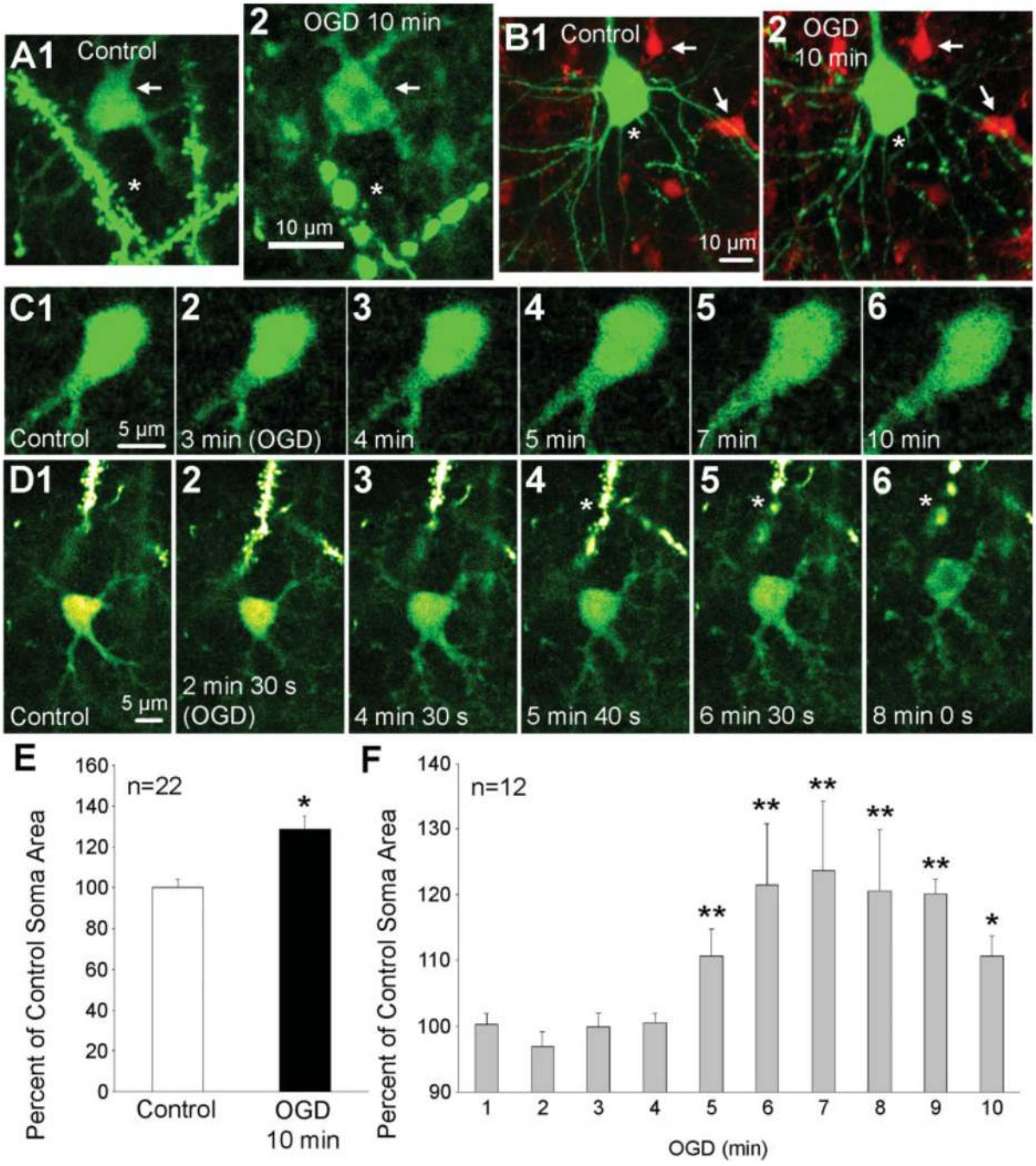

Fig. 4.

Astrocytes and neurons swell and dendrites bead in response to oxygen/glucose deprivation. **A1,A2**: 2PLSM images of a GFP-expressing astrocyte (arrow) and dendrites (asterisk) from CA1 region before (A1) and after 10 min exposure to OGD, resulting in astroglial soma swelling and dendritic beading (A2). The region is cropped to show the same field before and after OGD. **B1,B2**: 2PLSM images of a GFP-expressing neuron (green) and astrocytes stained with SR101 (red) in a slice from somatosensory cortex. The neuronal (asterisk) and astroglial somata (arrows) seen in control (B1) become swollen and dendrites bead as the entire field expands during 10 min of OGD (B2). **C1—C6**: 2PLSM time sequence of a GFP-expressing astrocyte from CA1 during OGD. Time of OGD exposure is indicated within each image. The

soma is swollen within 5 min (C4) and remains swollen for the entire 10 min exposure (C6). **D1—D6**: 2PLSM time sequence of an astrocyte and adjacent dendrite exposed to OGD (control in D1; subsequent images show time stamps during 10 min of OGD). The astrocyte swells around 4.5 min (D3) and the dendrite beads during the next minute (asterisks; D4—D6). **E**: Summary from 22 astrocytes in 10 slices from 6 animals showing the effect of 10 min of OGD on astroglial soma area. Values are shown as percent of control. Asterisk indicates significant difference from control (*$P < 0.001$). **F**: Graph of the events depicted in C showing the time-course of astroglial soma swelling during OGD. Values are shown as percent of control. Asterisk indicates significant difference from control (*$P < 0.05$, ** $P < 0.01$).

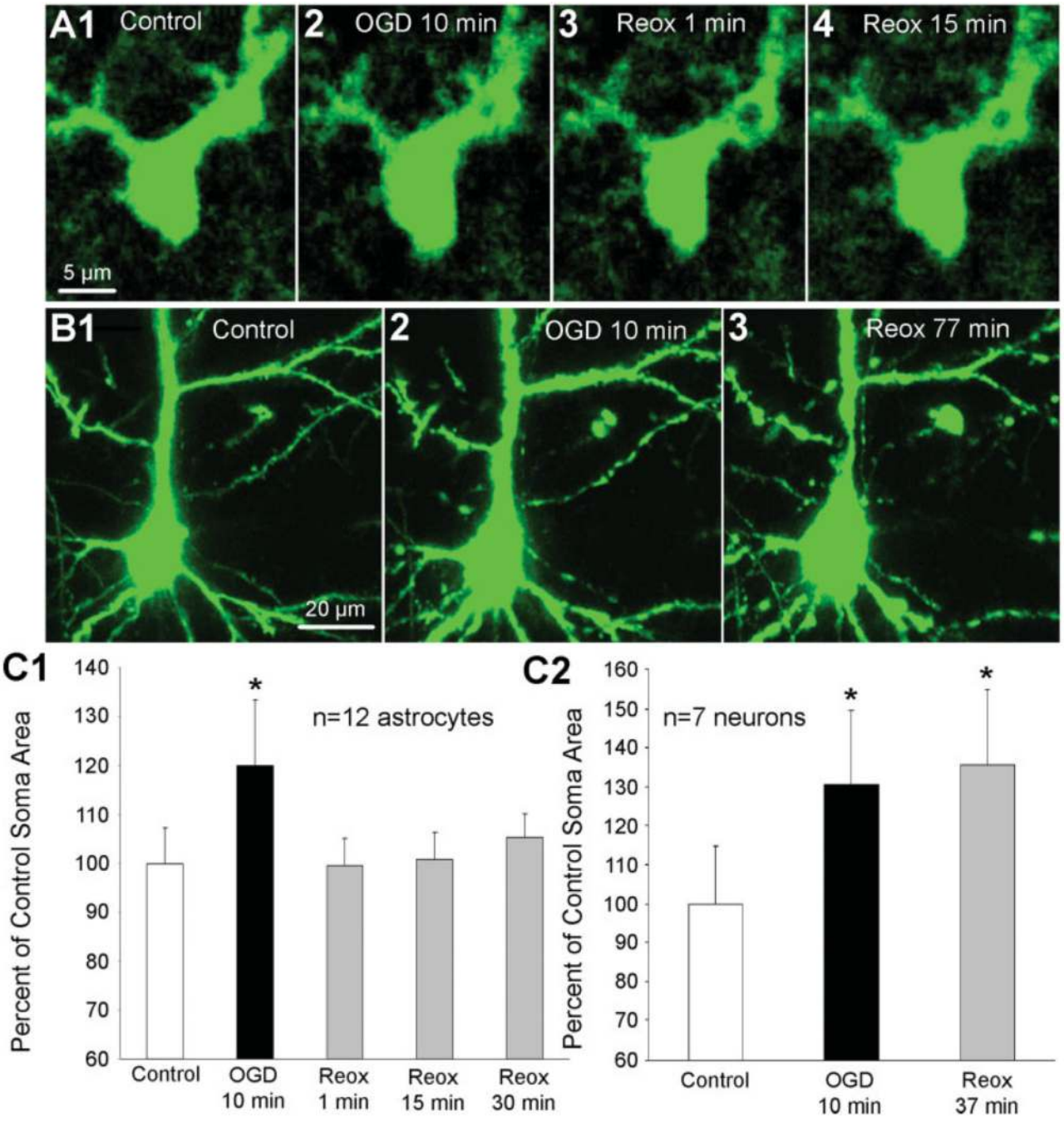

Fig. 5.

Astrocytes, but not neurons, show recovery from OGD-induced swelling in cortical slices. **A1—A4**: 2PLSM sequence of a GFP-expressing astrocyte from CA1 region of hippocampal slice. The astroglial soma (A1, control) swells during 10 min of OGD (A2). The swelling rapidly reverses during 1 min of exposure to control ACSF (A3), and volume remains constant during the next 15 min of re-oxygenation (A4). **B1—B3**: 2PLSM sequence of a GFP-expressing pyramidal neuron. The neuronal soma (B1, control), swells during 10 min of OGD (B2) but does not recover following 77 min of re-oxygenation (B3). **C1**: Summary from 12 astrocytes in 9 slices from 5 animals showing the effects of 10 min OGD and subsequent re-oxygenation/ normoglycemia on astroglial soma area. Values are shown as percent of control. Asterisk

indicates significant difference from control (*$P < 0.01$). **C2**: Summary from 7 neurons in 7 slices from 6 animals showing the effects of 10 min OGD and subsequent re-oxygenation (36.7 ± 26.5 min) on neuronal soma area. Values are shown as percent of control. Asterisks indicate significant difference from control (*$P < 0.001$).

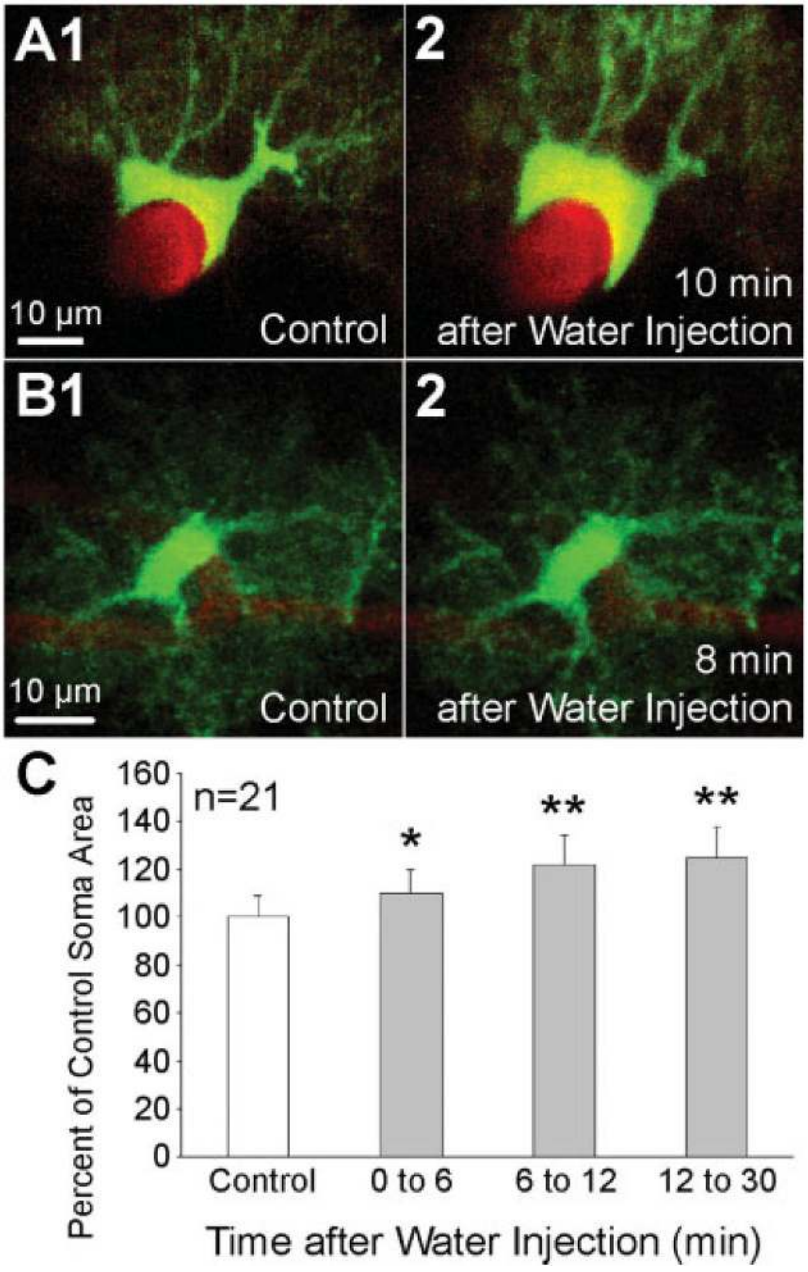

Fig. 6.

Astrocytes swell *in vivo* following intraperitoneal water injection. **A1,A2**: 2PLSM images of an astrocyte (green) from layer II/III of somatosensory cortex with the soma surrounding a blood vessel (red) labeled with Texas Red dextran. The astrocyte (A1, control) is swollen at 10 min after IP water injection (A2). **B1,B2**: An astrocyte whose soma does not directly contact a blood vessel (but does make contact via end-feet, confirmed by following processes in z-series) is swollen by 8 min after water injection. **C**: Summary from 21 astrocytes from 10 animals showing increase in astroglial soma area following water injection. Values are shown as percent of control. Asterisk indicates significant difference from control (*$P < 0.05$, **$P < 0.001$).

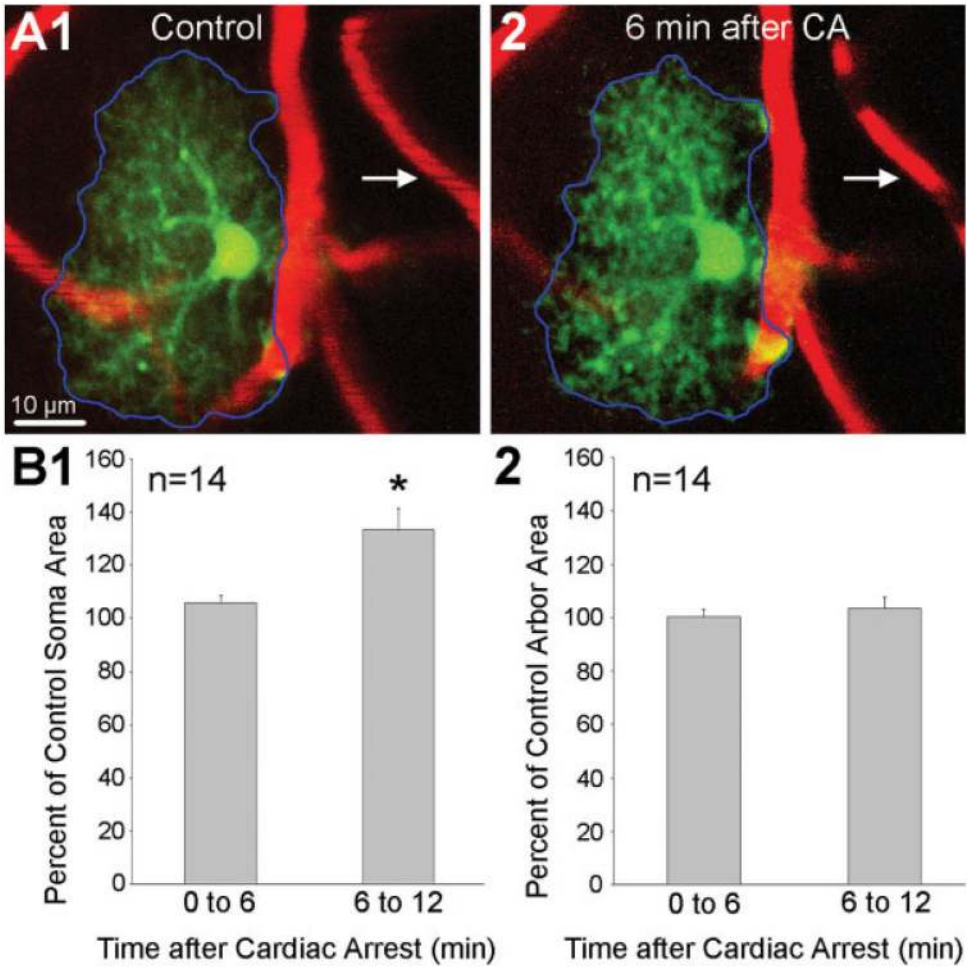

Fig. 7.

Astrocytes swell *in vivo* following global ischemia induced with cardiac arrest by air embolization. **A1,A2**: 2PLSM images of an astrocyte (green) from layer II/III of somatosensory cortex and blood vessels (red). Blood flow within a capillary in control (A1, arrow) is indicated by streaking caused by scanning of moving non-fluorescent red blood cells. Blood flow stalls following cardiac arrest (A2, arrow) accompanied by swelling of astroglial soma and processes. Despite process swelling (A2), the area of the astroglial arbor remains constant. The blue outline (A1,A2) indicates the perimeter of the visible astroglial domain. **B1**: Summary showing an increased astroglial soma area after global ischemia. Values are percent of control from 14 astrocytes from 6 animals. Asterisk indicates significant difference from control ($*P < 0.01$). **B2**: Summary of measurements of the same astrocytes from B1, showing constant area of the astroglial arbor following global ischemia ($P = 0.808$). Values are shown as percent of control.